Production of Hydrogen by Steam Oxidation of Calcium Ferrite Reduced with Various Coals

Ranjani Siriwardane*[1], James Poston[1], Esmail Monazam [1,2] and George Richards[1]

1 U.S. Department of Energy, National Energy Technology Laboratory, 3610 Collins Ferry Road, P.O. Box 880, Morgantown, WV 26507-0880

2 REM Engineering Services, PLLC, 3537 Collins Ferry Road, Morgantown, WV 26507-0880

* Corresponding author:

Ranjani Siriwardane

U.S. Department of Energy

National Energy Technology Laboratory

3610 Collins Ferry Road

P.O. Box 880

Morgantown, WV 26507-0880

Tel.: + 01-304-285-4513

Fax: + 01-304-285-0903

E-mail: ranjani.siriwardane@ netl.doe.gov

Highlights

- Hydrogen production by steam oxidation of reduced $CaFe_2O_4$ demonstrated
- High conversion (>75%) of steam to hydrogen demonstrated
- Lignite and sub-bituminous coals showed the best reduction rates of $CaFe_2O_4$
- Scaling up the production of $CaFe_2O_4$ was successful
- A 25-cycle test of H_2 production with steam/reduced $CaFe_2O_4$ showed stable performance

ABSTRACT

Production of H_2 by steam oxidation was demonstrated with calcium ferrite ($CaFe_2O_4$) after coal gasification to produce CO with several types of coals. All coal types reacted with $CaFe_2O_4$ to produce CO. The reduced $CaFe_2O_4$ after the reaction with coal can also be oxidized with steam at 800 $^{\circ}$C while producing of H_2. Sub-bituminous coal and lignite coal had better reactivity with $CaFe_2O_4$ than the bituminous coal. A ten-cycle test conducted with Wyodak coal/$CaFe_2O_4$ at 800 $^{\circ}$C showed stable production of H_2 during oxidation with steam. A 25-cycle steam oxidation test conducted after reduction of $CaFe_2O_4$ with lignite coal also showed a very stable performance. Steam oxidation is sufficient for maintaining the cyclic reactions. A larger scale (2 kg batch) production of $CaFe_2O_4$ by wet granulation-tumbling method was successful. Steam oxidation was demonstrated with the large-scale batch of $CaFe_2O_4$ after reduction with Wyodak coal

Keywords: chemical looping H_2 production, oxygen carriers for H_2 production, production of H_2 with coal/oxygen carriers.

1.0 INTRODUCTION

Hydrogen is a promising energy source that is also environmentally benign. This valuable material is also used in oil refineries, for ammonia, methanol production and fuel cells. In recent years, the production of hydrogen from coal or methane has received attention. Coal gasification is currently the most popular commercial method of producing hydrogen from coal, but synthesis gas produced this way must be further processed in a water-gas shift reactor (WGS) to produce a gas stream containing H_2 and CO_2. [1-4]. An additional pressure swing adsorption (PSA) step is required to separate CO_2 and H_2 to produce pure H_2 and sequestration-ready CO_2. In addition, to produce a concentrated syngas free of nitrogen, conventional coal gasification techniques require an air separation unit to obtain pure oxygen [5]. Therefore, alternative technologies that eliminate the WGS, PSA and air separation unit are desirable for production of H_2 from coal, specifically for the operation of small-scale coal gasification units

Chemical looping gasification (CLG) is one of the technologies that uses oxygen from an oxygen carrier, such as a metal oxide, for the gasification of fuel to produce syngas. The reduced metal oxide oxygen carrier is then oxidized using air. CLG has been used for gasification of solid fuels such as coal, biomass and derived cokes for the generation of synthesis gas [6-16]. Calcium oxide decorated iron oxide [6] has been used to enhance the coal-steam gasification to produce syngas with H_2/CO ratio of 12:1 in a fluidized bed reactor. Fe-Ni bimetallic oxygen carriers have shown promising performance for chemical looping gasification of biomass in a 10 kWth interconnected circulating fluidized bed reactor [8]. Calcium sulfates [9,10] have been used to increase the rate of coal-steam gasification but the syngas yields were low in the presence of the oxygen carrier. Studies in dual fluidized bed reactor indicated that the bi metallic oxygen carriers such as FeTiO3, Mn_{1-x} Cu_xO_y and Mn_{1-x} Fe_xO_y may be suitable oxygen carriers for coal gasification [11]. A theoretical study on the relationship between electronic properties of Fe_3O_4 substituted by Ca and

Ba and their reactivity in chemical looping process has shown that these substitutions enhanced the reactivity of the iron oxide oxygen carriers [14]. An iron based oxygen carrier (OC) developed from bauxite residual from alumina industry has shown sufficient activity to transport oxygen and heat from the air reactor to gasifier to promote gasification [15]. These reported CLG processes require steam in addition to the oxygen carrier for fuel gasification. Selection of oxygen carriers for the process has been difficult because most oxygen carriers react with syngas initially produced by coal-steam gasification even though they enhance the gasification rates, and it has been difficult to stop the reaction at the syngas stage.

As described in our previous studies [16], $CaFe_2O_4$ and $BaFe_2O_4$ selectively react with coal to produce CO but have minimal reactivity with CO, making them very desirable as oxygen carriers for CLG processes. Steam is not required for gasification of coal with $CaFe_2O_4$ and $BaFe_2O_4$ oxygen carriers unlike with the other oxygen carriers reported in the literature. According to the data reported in the Ellingham diagram [17], there are very few metal oxides in the syngas production range. According to calculations based on use of FactSage software, the free energies of oxidation of reduced $CaFe_2O_4$ components such as CaO, Fe^0, FeO to produce $CaFe_2O_4$ are in the range of syngas production in the Ellingham diagram at 700-900 $^{\circ}$C. Our previous studies [16, 18] also showed that reactions proceed via solid-solid interactions. We have also reported kinetic studies [18] of the interactions between the solid chars with these unique metal ferrites.

In CLG, solid-solid interactions between coal and the oxygen carrier play a key role. Therefore, fixed-bed gasifier designs already established in industry, [19,20], could be used in a commercial process. Moving-bed gasifiers may also be used with both solids moving together. Solid contact between the coal char and oxygen carrier must occur to ensure that oxygen can be transferred directly via proximal contact - the rate-limiting factor for solid fuel conversion [18, 21, 22].

CLG technologies arose from parent process concepts, such as coal direct chemical looping combustion (CLC). In chemical looping combustion processes, oxidation of the reduced oxygen carrier is traditionally conducted using air, which generates heat for various processes (23-31). In addition to oxidation of reduced oxygen carriers in CLC with air to generate heat, oxidation of reduced iron-based oxygen carriers by steam to produce H_2 has also been reported by various researchers [32-36]. Steam -iron process [32] to produce H_2 by steam oxidation of iron has been used commercially to produce H_2 and the process required initial reduction of iron oxide by a strong reducing gas such as syngas. Continuous high purity hydrogen generation for 300 hrs. been demonstrated in a 25 kWth sub-pilot unit by a chemical looping process which included reduction of iron oxide with syngas and oxidation with steam [33]. A techno-economic analysis of coal-based hydrogen and electricity cogeneration processes with CO_2 Capture indicated that the syngas chemical looping strategies have the potential to notably reduce the energy and cost penalties for CO_2 capture in coal conversion processes. In this process, syngas produced by coal gasification was used for reduction of an iron-based oxygen carrier prior to oxidation of the reduced oxygen carrier with steam [34]. Another techno-economic analysis on conversion of brown coal to hydrogen and power based on enhanced process integration of coal direct chemical looping, combined cycle and hydrogenation showed promising results [35]. Modification of iron oxide oxygen carrier with potassium has shown improved performance [36].

In our previous studies [16,18] oxidation of reduced $CaFe_2O_4$, which contained phases CaO, Fe, and FeO after the reaction with coal, was conducted with air, which is highly exothermic, and re-formation of CaFe2O4 during oxidation was demonstrated. Another important property of this material is that the reduced $CaFe_2O_4$ can also be oxidized with steam to produce H_2. Deep reduction of $CaFe_2O_4$ required prior to steam oxidation can be performed by direct reaction with coal at 800-

850 ^{0}C, unlike that with iron oxide which requires a strong reducing gas such as syngas for initial reduction as reported in the previous studies. Production of hydrogen via steam oxidation of $CaFe_2O_4$ after reduction with coal is reported in this work. CLG with $CaFe_2O_4$ with several types of coal such as Wyodak, Power River Basin (PRB) and Mississippi lignite and oxidation with steam for H_2 production were investigated. Stability of production of H_2 via steam oxidation of the reduced $CaFe_2O_4$ with both sub-bituminous Wyodak coal and lignite coal during a multi cycle tests is also reported. In addition, a 2kg batch of $CaFe_2O_4$ prepared using a wet granulation/tumbling process that could be easily scaled up for commercial scale preparation was demonstrated. The test results from the large-scale $CaFe_2O_4$ batch/ Wyodak coal and steam oxidation to produce H_2 are also reported.

EXPERIEMENTAL

2.0 MATERIALS AND METHODS

2.1 Materials

CaO (99%, Aldrich) and Fe_2O_3 (99.99%) were used for the preparation of $CaFe_2O_4$. The powders were mixed, and enough water was added for pelletization during mixing. The mixture was calcined at 1000 °C for 6 hours. Wyodak coal, Power River Basin coal (PRB), Mississippi coal and Texas bottom seam coal were used. The analysis data of the coals are listed in Table 1. Coal was mixed physically with the oxygen carriers by a mass ratio (oxygen carrier mass to coal mass) corresponding to the stoichiometric oxygen supply to produce CO. Stoichiometric conditions are used here to demonstrate the minimum oxygen carrier required for converting the solid carbon. As explained above, and in [16], excess oxidant has minimal reaction with gas-phase CO because of thermodynamics. The particle size of coal was in the range of 75-300 μm, and the

oxygen carrier had a particle size range of 53 -125 µm. A large-scale (1.5 kg) batch was prepared using a similar procedure.

Table 1: Proximate and Ultimate Analysis of Coals

Analysis	Component (%wt.)	Wyodak Coal (Subbituminous)	Powder River Basin (PRB) (Subbituminous)	Mississippi Lignite	Texas Bottom Seam (Subbituminous)
Proximate	%Moisture	NA, dry basis	NA, dry basis	Na, Dry Basis	Na, Dry Basis
	%Ash	7.57	8.83	25.71	15.81
	%Vol. Matter	44.86	40.83	43.76	47.4
	%Fixed Char	47.57	50.34	30.53	36.79
Ultimate	%Ash	7.57	8.83	25.71	15.81
	%Carbon	69.77	67.24	51.75	62.53
	%Hydrogen	5.65	4.23	3.57	4.74
	%Nitrogen	0.94	1.53	1.27	1.23
	%Total Sulfur	0.43	0.38	0.73	0.99
	%Oxygen (diff)	15.64	17.79	16.97	14.69

2.2 Bench-Scale Fixed-Bed Flow Reactor Studies

2.2.1 Single-cycle tests with various coals

Bench-scale fixed-bed flow reactor (inner diameter 7 mm) tests were conducted with 4.5g $CaFe_2O_4$ and 0.6 g of coal. The outlet gas compositions (CO_2, H_2, CH_4 and CO) from the reactor were measured using a MS (Pfeiffer Omnistar). Helium was used as the inert flow gas because the mass spectral peaks for N_2 overlap with those of CO. The sample was heated in He at a flow rate

of 100 cm3/min (0.1 L/min) from ambient to 850 °C (ramp rate of 4 °C/min) and kept isothermal at 850 °C for 60 min. After the gasification step, the sample was exposed to steam/He.

2.2.2 Ten-cycle test with Wyodak coal and $CaFe_2O_4$ with steam introduction at 800 °C

Ten-cycle bench-scale fixed-bed flow reactor (inner diameter 7 mm) tests were conducted with a 4.5 g sample of $CaFe_2O_4$ and 0.6 g of Wyodak coal. The sample was heated in He at a flow rate of 100 cm3/min (0.1 L/min) from ambient to 800 °C (ramp rate of 4 °C/min) and kept isothermal at 800 °C for 60 min. After the gasification step, the sample was exposed to 15% steam/He for 60 min at 800 °C. When the H_2 concentration was less than 500 ppm after reaching the maximum, the sample was cooled to 750 °C and air was introduced for oxidation.

2.2.3. 25-cycle tests with Lignite coal 30% steam 1.2 g lignite coal 9 g Ca ferrite 800 C

25-cycle bench-scale fixed-bed flow reactor (inner diameter 7 mm) tests were conducted with a 9 g sample of $CaFe_2O_4$ and 1.2 g of lignite coal. The sample was heated in He at a flow rate of 100 cm3/min (0.1 L/min) from ambient to 800 °C (ramp rate of 4 °C/min) and kept isothermal at 800 °C for 60 min. After the gasification step, the sample was exposed to 30% steam/He at 800 °C. When the H_2 concentration was less than 500 ppm after reaching the maximum, the sample was cooled to 750 °C and air was introduced for oxidation.

2.2.4 Test with the large-scale batch of $CaFe_2O_4$ and Wyodak coal

Bench-scale fixed-bed flow reactor (inner diameter 6 cm) tests were conducted with a 200-300 g sample of CaFe2O4 (particle size 53-125 micron) and 40 g of Wyodak coal (74- 300 micron).

The sample was heated in He at a flow rate of 8.4 scfh (3.95 L/min) from ambient to 800 °C (ramp rate of 4 °C/min). When the CO level was low (less than 500 ppm) after reaching the maximum, 15 % steam/He was introduced at 800 ˚C.

2.2.5 Scanning Electron Microscope with Energy Dispersive Spectroscopy (SEM-EDS)

JEOL-840A SEM interfaced to a Noran NS-6 X-ray microanalysis system was used for the analysis. The JEOL-840A has an annular backscatter detector (BSED), an ET type secondary electron detector (SED), and a Noran Ultra-Dry Energy Dispersive Spectrometer (EDS). The JEOL 840A SEM was routinely operated in a pressure range of 10-6 -10-5 Torr (1.3x10-5 to 1.3x10-6 Pa; 1 Torr ≈ 1.3224 Pa).

2.2.6 X-ray Diffraction (XRD)

XRD was performed in a Panalytical X'pert Pro Powder X-ray diffraction system with an Anton Par Hot Stage (Model# HTK-1200N) connected to a Eurotherm (Model# 2604) temperature controller. The XRD system has a Cu anode X-ray source (Cu kα = 1.5544 Å) and a PiXcel1D strip detector. The X-ray generator voltage and current was set at 45 kV and 40 mA respectively for sample analysis.

3.0 RESULTS AND DISCUSSION

3.1 Fixed bed flow reactor studies with Mixtures of $CaFe_2O_4$/several types of coal with 15% steam introduction at 850 ˚C

The results with Mississippi lignite coal and sub-bituminous PRB, Texas and Wyodak coals are shown in Figure 1. During the temperature ramp, coal reacted with $CaFe_2O_4$ to form CO as the

main product with some CO_2 while reducing $CaFe_2O_4$. When steam was introduced at 850 °C after the temperature ramp of coal/ $CaFe_2O_4$ in He, a significant amount of H_2 was observed.

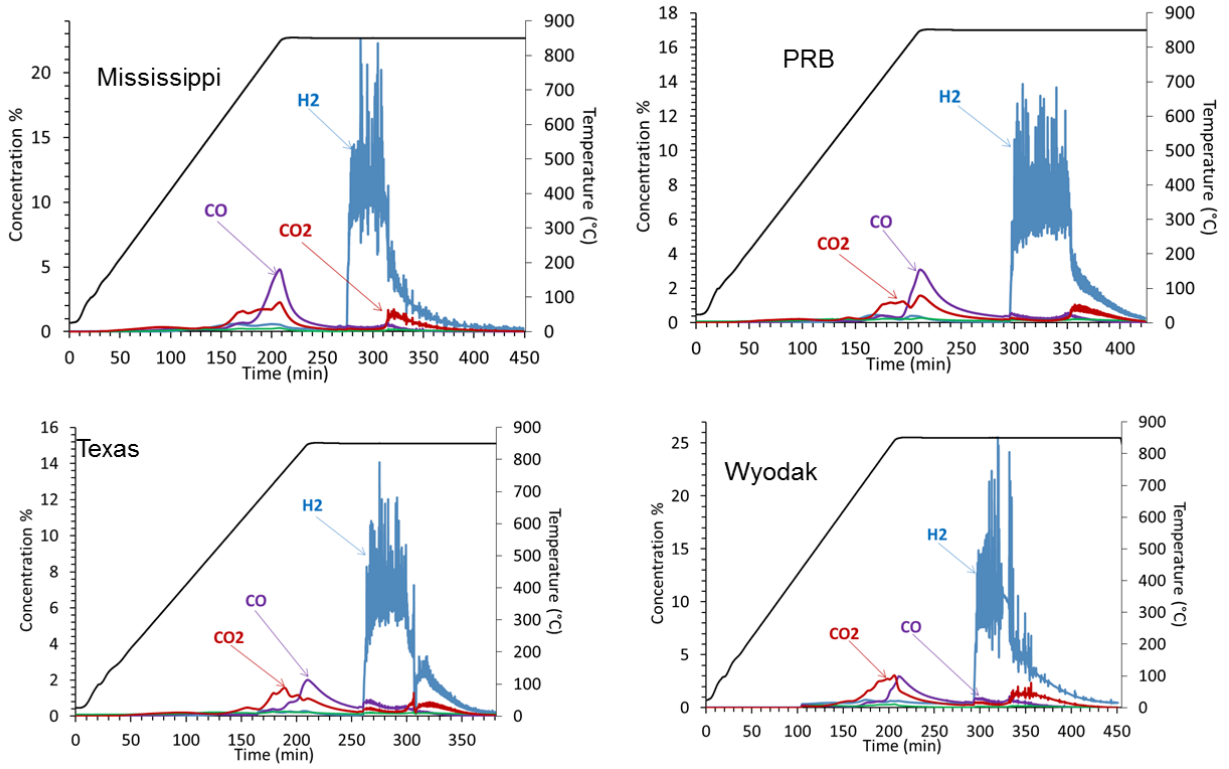

Figure 1: Effluent gas concentrations during temperature ramp of PRB coal/ $CaFe_2O_4$ in helium and introduction of 15% steam at 850 ˚C.

When air was introduced to the $CaFe_2O_4$ at 850 °C after introduction of steam, the consumption of oxygen was significantly lower than when air was introduced directly to the reduced $CaFe_2O_4$ without steam oxidation. This data indicated that the reduced $CaFe_2O_4$ was oxidized by steam while producing H_2. The bituminous coal, Illinois #6, did not have (not shown) high steam conversions to H_2 since the reduction rate of $CaFe_2O_4$ was low with Illinois coal (16,18). However, the lignite and sub-bituminous coals reacted with $CaFe_2O_4$ at a high rate which contributed to high H_2 at high production rate during steam oxidation.

3.5 Multi-Cycle Tests

3.5.1 Ten-cycle fixed bed flow reactor studies with $CaFe_2O_4$/Wyodak coal with 15% steam introduction at 800 °C followed by air introduction

During the ten-cycle test with 4.5 g $CaFe_2O_4$/0.6 g Wyodak coal, the initial temperature ramp was conducted in He. When steam was introduced to the reduced $CaFe_2O_4$ at 800 °C, a substantial amount of H_2 was observed. After each cycle, a new batch of 0.6 g of coal was added to the oxidized Ca ferrite oxidized from the previous cycle. The concentration of H_2 data when steam was introduced at 800 °C during the ten-cycle test is shown in Figure 2. A very stable production of H_2 was observed during the ten-cycle test. The maximum conversion of steam to H_2 was about 75%. The rate of H_2 production via oxidation of the reduced Ca Ferrite is significantly faster than the H_2 production via coal gasification with steam at 800 °C, as also shown in Figure 2.

The oxygen consumption data during air oxidation after the steam introduction at 800 °C is shown in Figure 3a. Comparative oxygen consumption data with air at 800 °C when steam was not introduced at 800 °C is shown in Figure 3b The oxygen consumption was lower with the sample that was exposed to steam at 800 °C prior to oxidation with air, which indicated that the reduced oxygen carrier was oxidized substantially with steam at 800 °C.

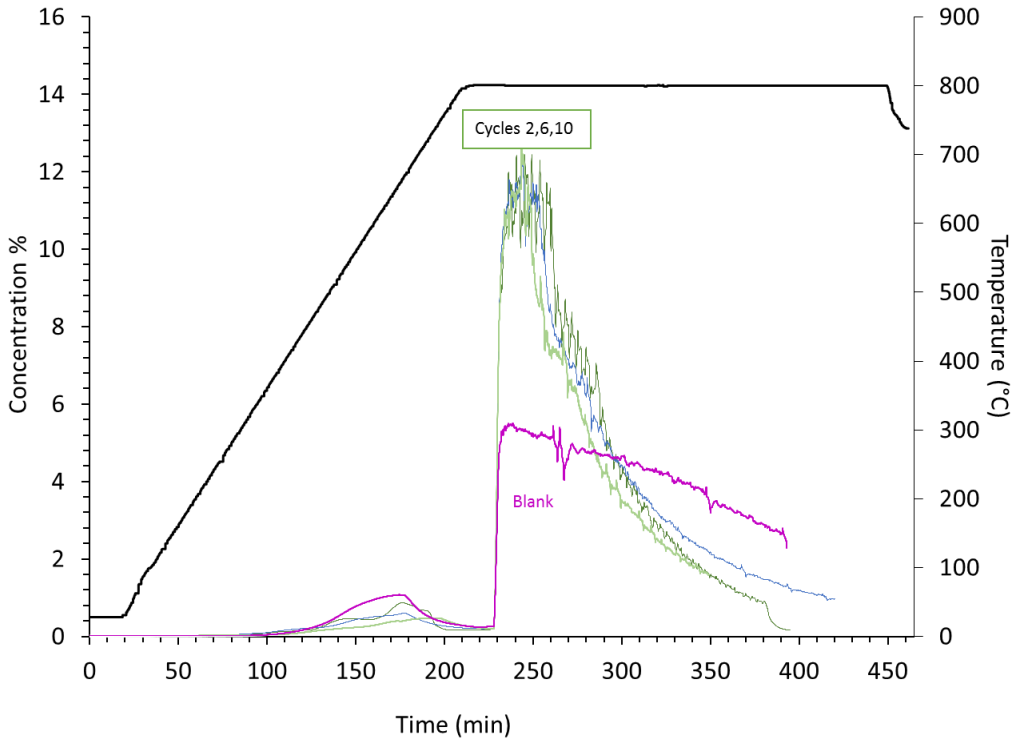

Figure 2: Concentration of H2 during the 10-cyle test of Wyodak coal/ $CaFe_2O_4$ with 15% steam introduction at 850 °C (for clarity only cycles 2,6 & 10 are shown)

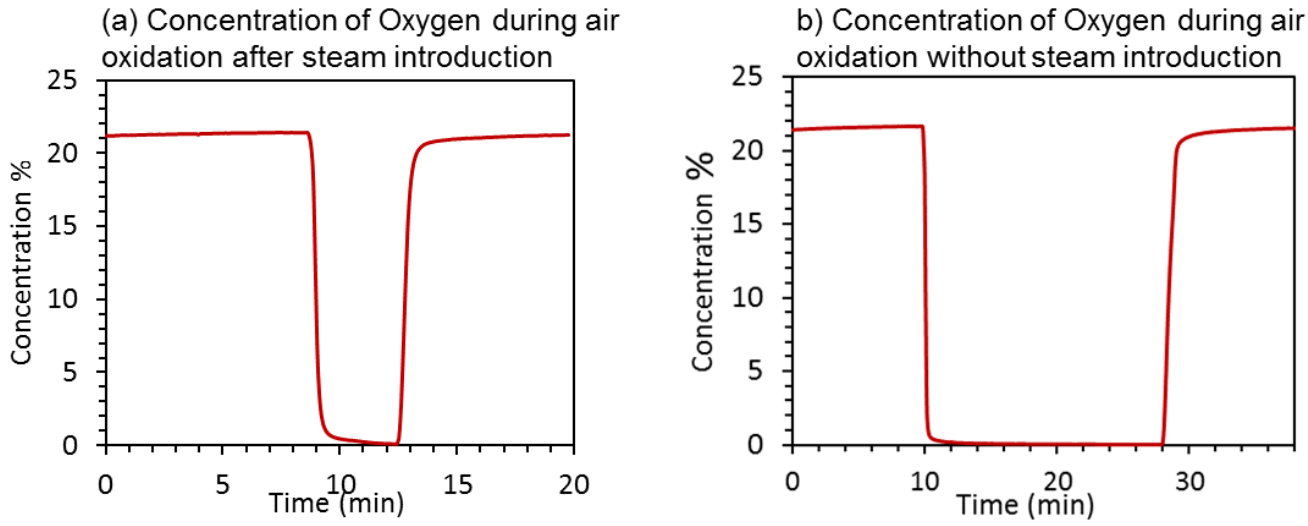

Figure 3: Concentration of oxygen during air oxidation with and without steam introduction after the temperature ramp of Wyodak coal /$CaFe_2O_4$ in Helium

3.5.1 Lignite coal 25-cycle test with steam oxidation and no air oxidation

During the 25-cycle test with 9 g $CaFe_2O_4$/1.2 g lignite coal, when 30% steam was introduced to the reduced $CaFe_2O_4$ at 800 °C after the initial temperature ramp in He, a substantial amount of H_2 was observed. In this test series, air oxidation was not conducted after steam oxidation. After each cycle, a new batch of 1.2 g of coal was added to the $CaFe_2O_4$ oxidized by only steam from the previous cycle. The concentration of H_2 data when steam was introduced at 800 °C during the ten-cycle test is shown in Figure 4. A very stable production of H_2 was observed during the ten-cycle test. The maximum conversion of steam to H_2 was about 75%.

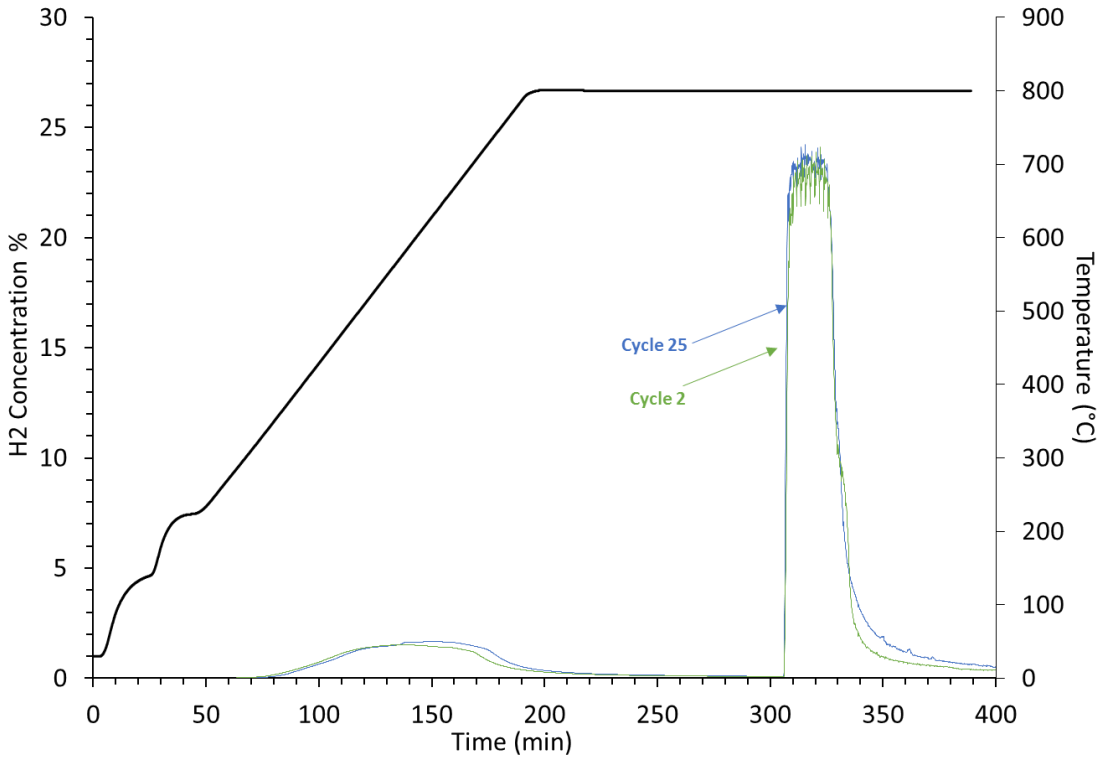

Figure 4: Concentration of H_2 during the 25-cyle test of lignite coal/ $CaFe_2O_4$ with 30% steam introduction at 800 °C (for clarity only cycles 2 & 25 are shown)

3.5.1.1 Oxidation rate analysis during the 25-cycle steam oxidation test with Ca ferrite after reaction with lignite coal

The weight gain by reduced Ca ferrite during oxidation with steam was calculated by assuming that one mole of atomic oxygen is added to the reduced Ca ferrite for every mole of H_2 produced. Therefore, the mass gained by reduced $CaFe_2O_4$ that caused by steam oxidation can be calculated with the following equation (1):

$$\Delta m(gain) = MW_O \times mol(H_2) \qquad (1)$$

where MW_O is the molar weight of atomic oxygen and $\Delta m(gain)$ is the measure of the total oxygen mass (g) gained by the reduced Ca ferrite by steam oxidation. The *mol*(H_2) represent the moles of H_2 produced, which is equivalent to the moles of atomic oxygen consumed by reduced $CaFe_2O_4$. The *mol*(H_2) was obtained by integration of curves in Figure 4.

The conversion (*X*) during oxidation is defined as:

$$X = \frac{\Delta m_{gain}}{\Delta m_{gain}(total)} \qquad (2)$$

where $\Delta m(gain)$ is the mass gain by the partially oxidized Ca ferrite during oxidation (Eq. 1) at a given time, $\Delta m_{gain}(total)$ is the total experimental mass gain during steam oxidations at 800 °C.

The degree of oxidation conversion (*X*) of the reduced Ca ferrite as a function of oxidation time for selected cycles using 25% steam at 800 °C are shown in Figure 5. As demonstrated by Fig. 5, the oxygen uptake increased linearly with exposure time up to about 90% of the oxidation conversion. The oxidation process of metal has been reported to obey power rate law [37] as shown in equation (3):

$$X^n = k_n t \qquad (3)$$

where *X* is the conversion during oxidation, or oxygen uptake, *k* is the uptake rate constant and *t* is oxidation time, and *n* is the conversion exponent. Many representative oxidation uptakes correspond to different conversion exponents: 1 for linear, 2 for parabolic and 3 for cubic [37]. Following assessment of the conversion vs. oxidation time data, it was ratified that the linear dependence (*n*=1) provides the best fit to the oxidation uptake from the initial stage of oxidation.to 90% of conversion as shown in Figure 6. These results revealed that the diffusion

resistance through oxide layer did not control the overall rate throughout the oxidation time. Therefore, the oxide scale provides no resistance to diffusion pathway for oxidizing gas. After inspection of the oxidation uptake data at different cycles (up to 25 cycles) as shown in Figure 5 and 6, there was no clear deviation in trend detected with cycle number. In terms of the oxidation uptakes, the overall profiles for different cycles exhibit a similar trend at all cycles and times. Rate of conversion computed from the data in Figure 6 was 0.038 min^{-1}.

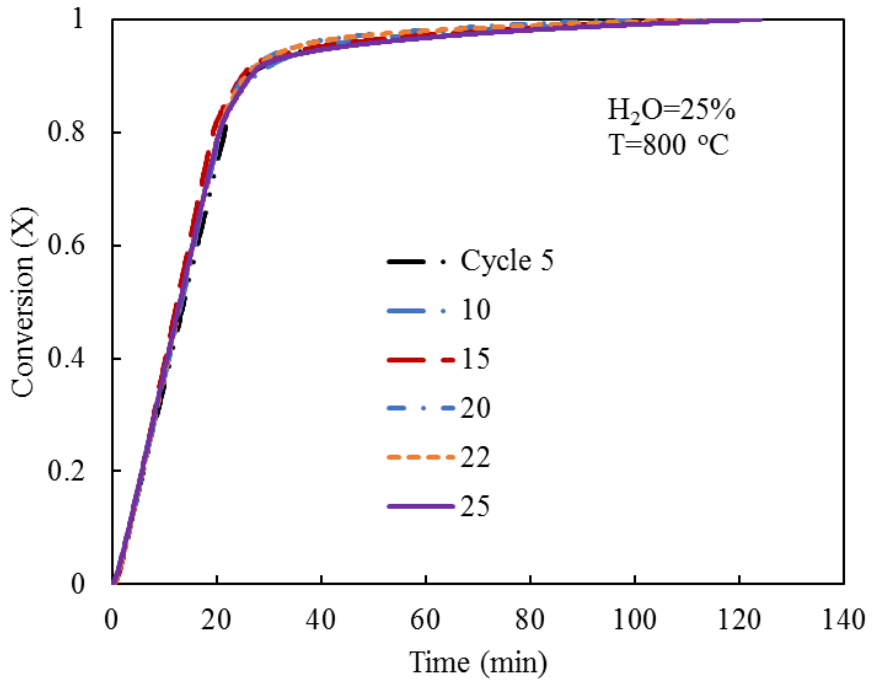

Figure 5: The degree of oxidation conversion (*X*) of reduced $CaFe_2O_4$ for different cycles at temperature 800 °C with 25% steam

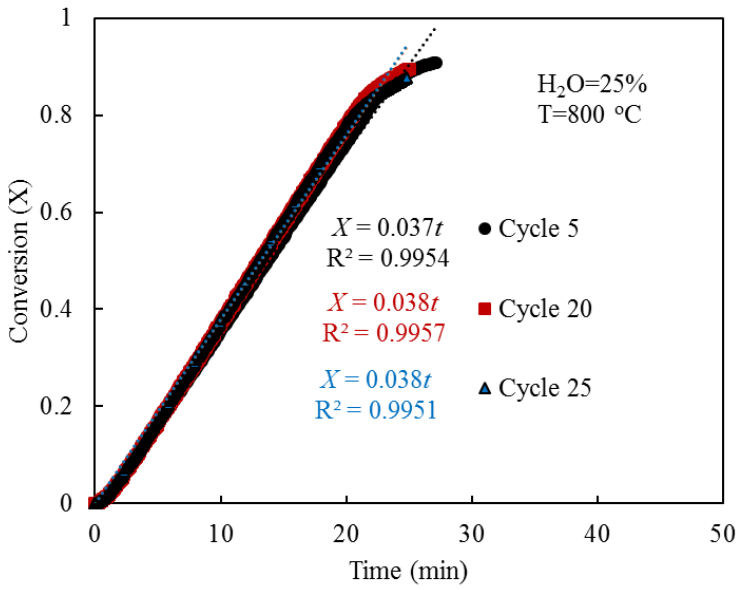

Figure 6: The linear dependence of oxidation conversion (*X*) of reduced $CaFe_2O_4$ with time (Eq. 3) using 25% steam and He balance and 800 °C

3.6 Fixed bed flow reactor studies with the large-scale batch of $CaFe_2O_4$

A 1.5 kg batch of $CaFe_2O_4$ was prepared using a wet agglomeration process. A 300 g of material sample in the size range 53-125 µm was mixed with 40g of the Wyodak coal and a temperature ramp was conducted to 800 °C in He. The concentrations of effluent gases measured using mass spectrometer during the temperature ramp are shown in Figure 7. The concentration of CO was the highest, and the gas compositions were very similar to what was observed with the small-scale tests shown in Figure 1.

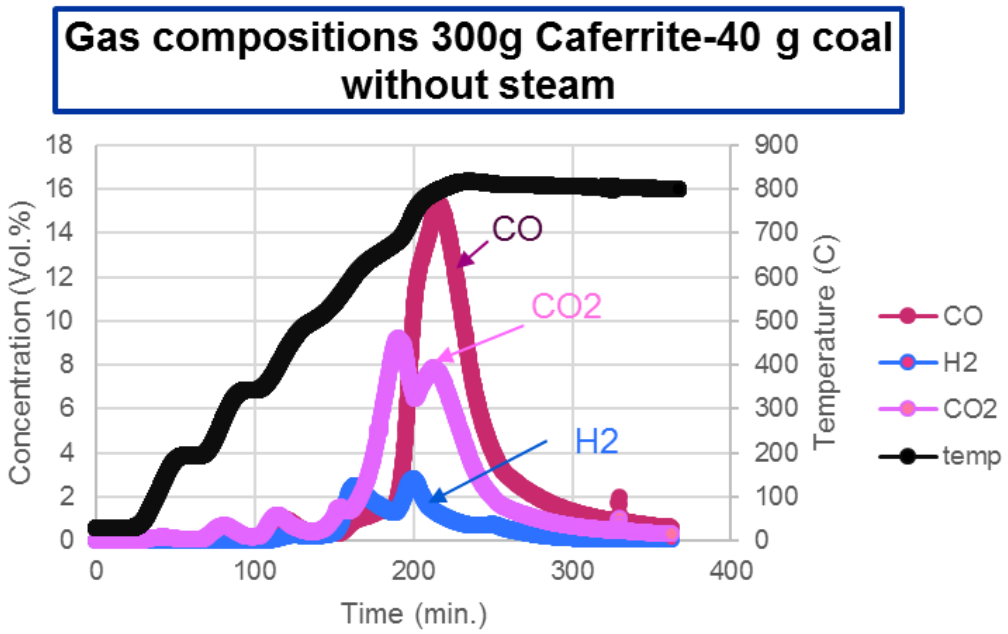

Figure 7: Effluent gas concentrations during temperature ramp of Wyodak coal/large scale $CaFe_2O_4$ batch in Helium

Steam oxidation was also conducted with the large-scale batch. After the temperature ramp with coal, steam was introduced at 800 ˚C to the reduced $CaFe_2O_4$. A substantial amount of H_2 was produced as shown in Figure 8, indicating that the reduced $CaFe_2O_4$ was oxidized by steam similar to the results found with the small-scale batch (Figures 1 and 2). The data confirmed that even with a large-scale batch, the reduced $CaFe_2O_4$ can be regenerated using steam to produce H_2. The major advantage with the $CaFe_2O_4$ oxygen carrier is that it can react with coal directly to produce CO and be oxidized with steam to produce H_2. The H_2 production data when 15% steam was introduced to Wyodak coal without $CaFe_2O_4$ is also shown in Figure 8 and it is lower than that with steam/reduced $CaFe_2O_4$.

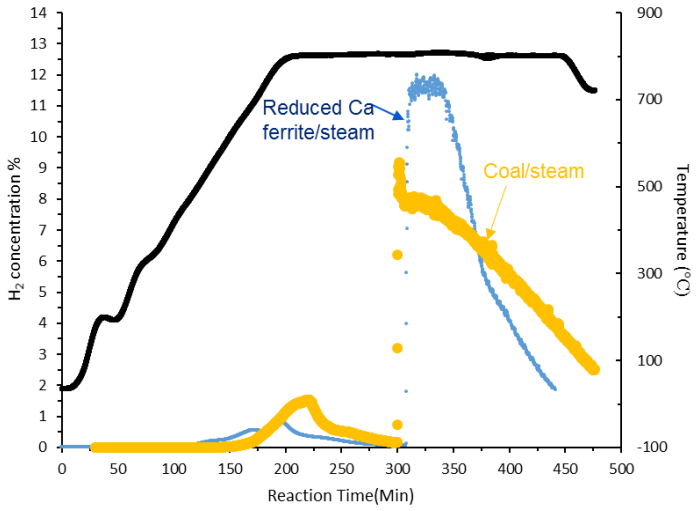

Figure 8: Concentration of H2 during the 15% steam introduction at 850 °C with Wyodak coal/ $CaFe_2O_4$

3.7 Characterization

3.7.1 Scanning Electron microscopy(SEM)/Energy dispersive analysis and X-Ray diffraction analysis

Scanning electron photo micrographs of fresh $CaFe_2O_4$ and after the 25th cycle oxidation with steam (section 3.5.1) following the reduction with lignite coal are shown in Figure 9. The SEM photomicrographs indicated that there was a change in the surface morphology after the cyclic reactions with coal and steam. The fresh sample appeared have larger grains and more porous than the reacted sample. Multi-cycle reduction via solid-solid interactions and oxidation with steam at 800 $^{\circ}$C have contributed to the morphology changes. Even though there were changes in the surface morphology, the reactivity of $CaFe_2O_4$ was stable during the 25-cycle test.

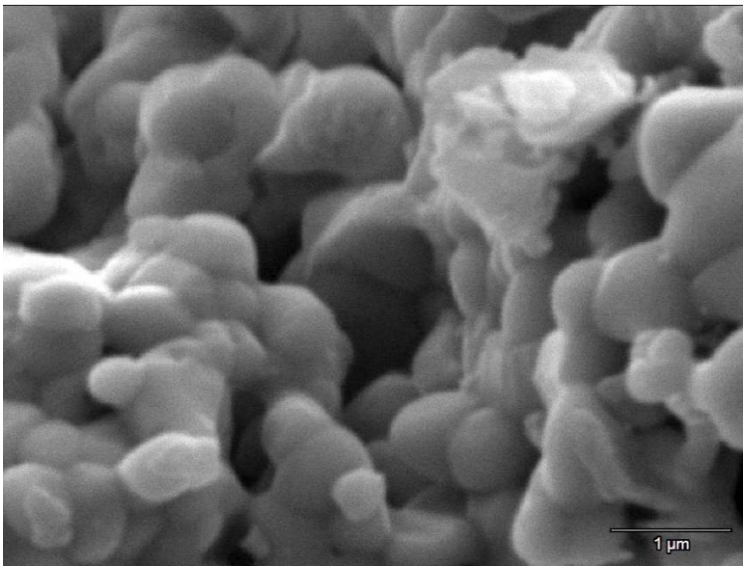

(A)

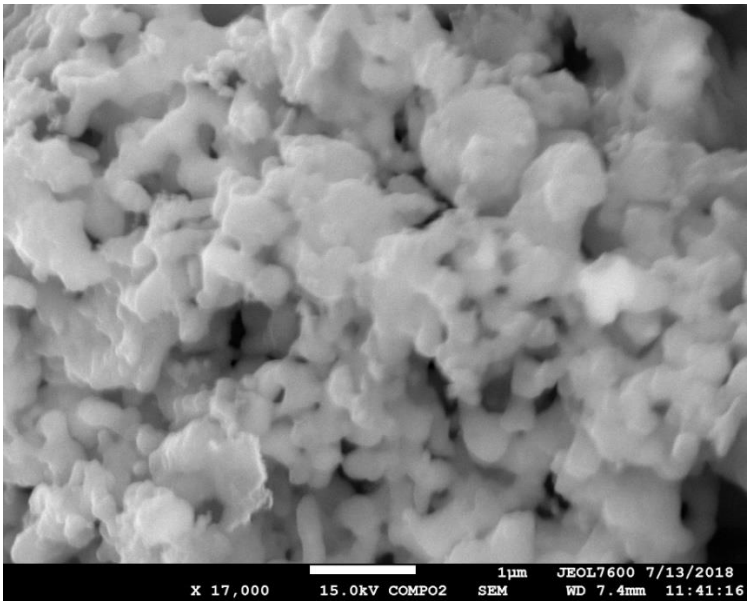

(B)

Figure 9: Scanning electron photomicrographs of (A) fresh $CaFe_2O_4$ and (B) after 25th steam oxidation cycle after reduction with lignite coal

3.7.2. X-Ray Diffraction Analysis

3.7.2.1 X-Ray Diffraction Analysis at ambient temperature

X-Ray diffraction (XRD) data of the fresh Ca ferrite indicated the presence of mainly the $CaFe_2O_4$ phase as shown in Figure 10. The reduced forms of $CaFe_2O_4$ after reduction with coal have been previously [18] identified as CaO, FeO and Fe^0. The XRD data after the 25^{th} oxidation with steam (described in section 3.5.1 with lignite coal), the peaks corresponded to $Ca_2Fe_2O_5$ (main) and Fe_3O_4. The data indicated that the reduced Ca ferrite after steam oxidation was only oxidized to $Ca_2Fe_2O_5$ phase not to the original $CaFe_2O_4$ phase.

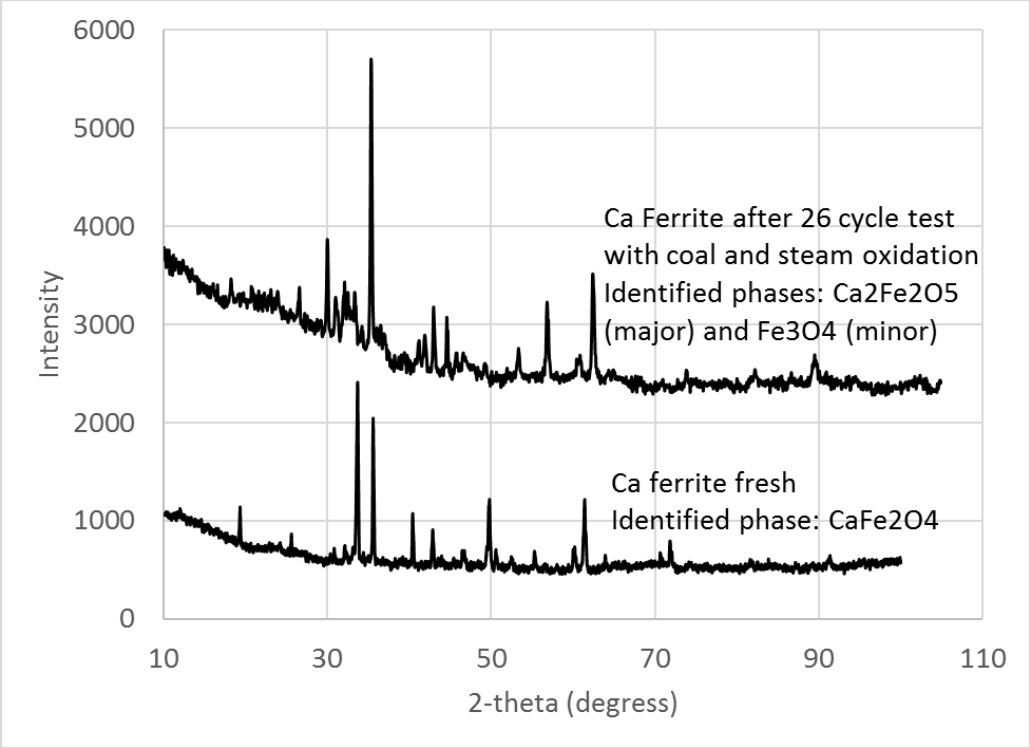

Figure 10: X-Ray diffraction data of ca ferrite fresh and after 25th cycle steam oxidation cycle-test with lignite coal/ $CaFe_2O_4$

However, when the oxidations are conducted with air instead of steam, the original $Ca_2Fe_2O_5$ was formed as reported previously [18]. The formation of $Ca_2Fe_2O_5$ after oxidation with steam did not impact the cyclic reactions because $Ca_2Fe_2O_5$ can be easily reduced by direct reaction with coal. After the first cycle, reduction of $Ca_2Fe_2O_5$ with coal and oxidation of reduced $Ca_2Fe_2O_5$ with steam to produce H_2 showed stable performance for the next 24 cycles.

3.7.2.1 In-Situ X-Ray Diffraction Analysis during temperature ramp with carbon – Ca ferrite and during steam exposures at 800 ^{0}C

A mixture of carbon (lamp black) and $CaFe_2O_4$ was placed in the hot stage of the XRD unit and temperature was ramped from ambient to 800 ^{0}C in nitrogen. The XRD data were obtained during the temperature ramp are shown in Figure 11. The initial phase at ambient temperature corresponded to $CaFe_2O_4$. After the temperature ramp to 850 C, main phases identified were Fe and CaO which indicated that $CaFe_2O_4$ was completely reduced to Fe and CaO.

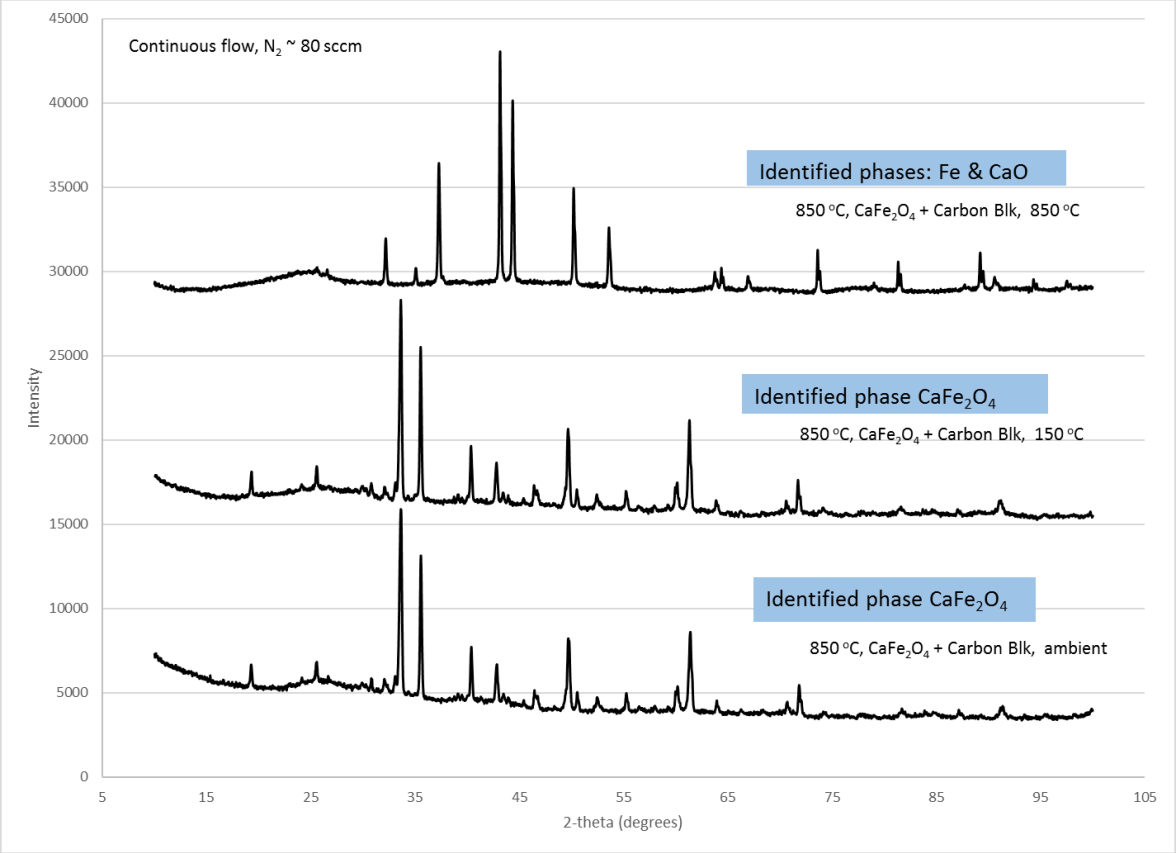

Figure 11: In-situ XRD data of ca ferrite -carbon mixture during the temperature ramp up to 850 ^{0}C

After the reaction with carbon in the XRD hot stage, steam was introduced to the sample and in-situ XRD data were obtained at 850 ^{0}C. Steam was introduced by flowing nitrogen at 80 sccm through a water bubbler. The data during the steam introduction is shown in Figure 12. The initial phases CaO and Fe changed to $Ca_2Fe_2O_5$ after the steam introduction and was not changed even after steam exposures overnight. The data are consistent with the ambient temperature XRD data with samples obtained after cyclic reactions described in the previous section (Figure 10).

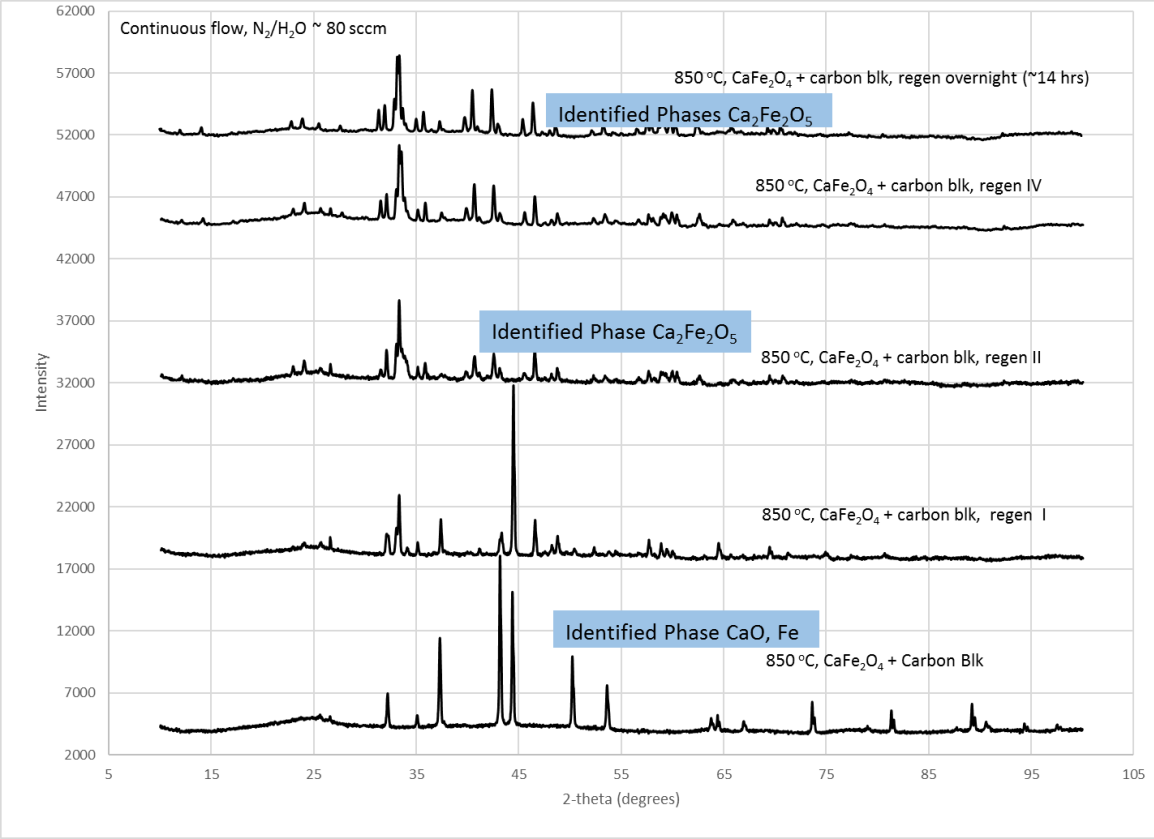

Figure 12: In-situ XRD data of reduced Ca ferrite during exposure to steam at 850 ^{0}C

4.0 Possible processes

According to the XRD data, the main phases formed after steam oxidation were $Ca_2Fe_2O_5$ and Fe_3O_4. So, the cyclic reactions can be described by equations (4) and (5).

$$3C + Ca_2Fe_2O_5 + Fe_3O_4 \rightarrow 3CO + 2CaO + 4FeO + Fe \;,\; \Delta H_{800} = 558\ KJ \quad (4)$$

$$2CaO + 4FeO + Fe + 3H_2O \rightarrow Ca_2Fe_2O_5 + Fe_3O_4 + 3H_2,\; \Delta H_{800} = -174\ KJ \quad (5)$$

The reduction of $Ca_2Fe_2O_5$ is endothermic, while the oxidation with steam is exothermic. The combined reaction is endothermic, and heat must be provided for the reaction. The heat may

be provided by oxidation of a portion of the reduced ca ferrite with air as shown in reaction (6), which will produce sufficient energy for the process.

$$CaO + FeO + Fe + O_2 \rightarrow CaFe_2O_4, \quad \Delta H_{800} = 619\ KJ \qquad (6)$$

Possible processes for generation of H_2 with coal/Ca ferrite are shown in Figure 13 and 14. In the process shown in Figure 11, a separate air oxidation reactor is used for production of necessary heat for the endothermic fuel reaction. Some of the reduced Ca ferrite from the fuel reactor is transferred to the air reactor for oxidizing with air to generate heat. In the process shown in Figure 12, air oxidation is performed after the steam oxidation to generate additional heat.

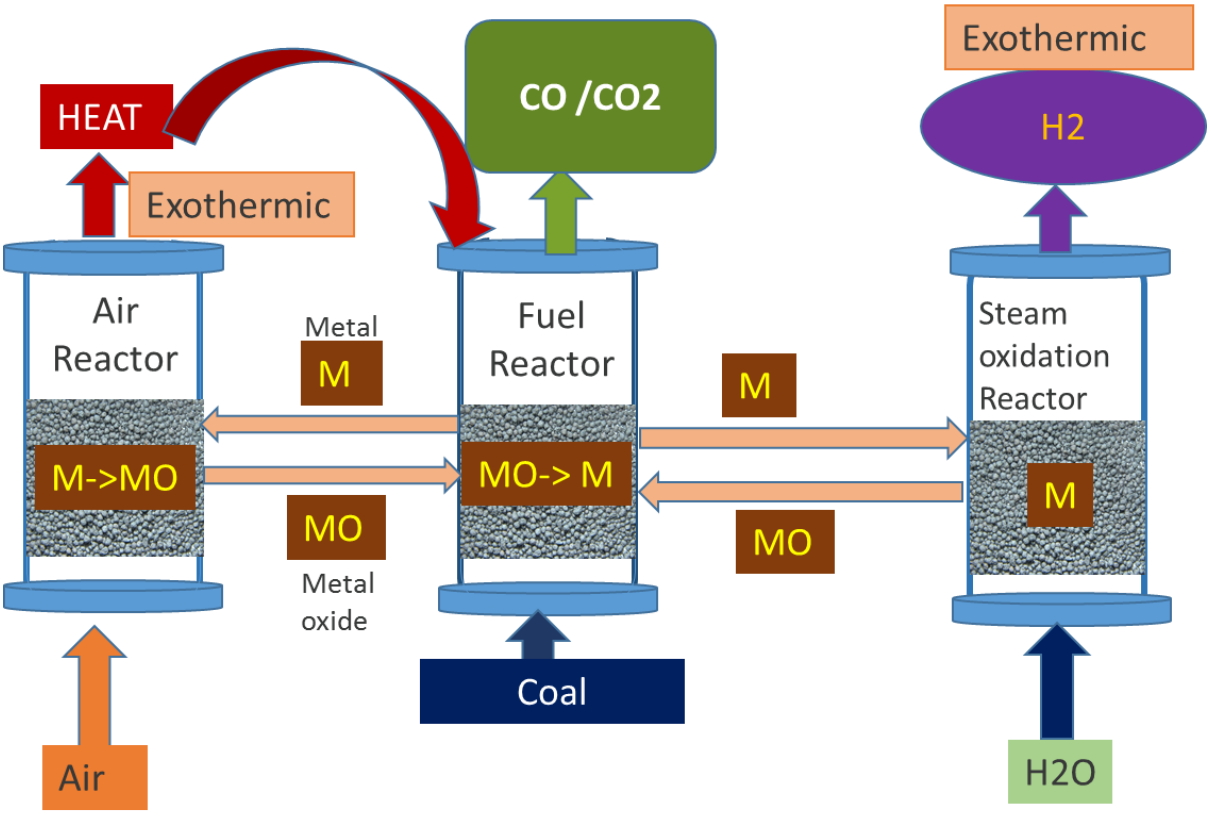

Fig 13: Process of production H_2 from steam oxidation of reduced Ca ferrite and air oxidation to produce heat

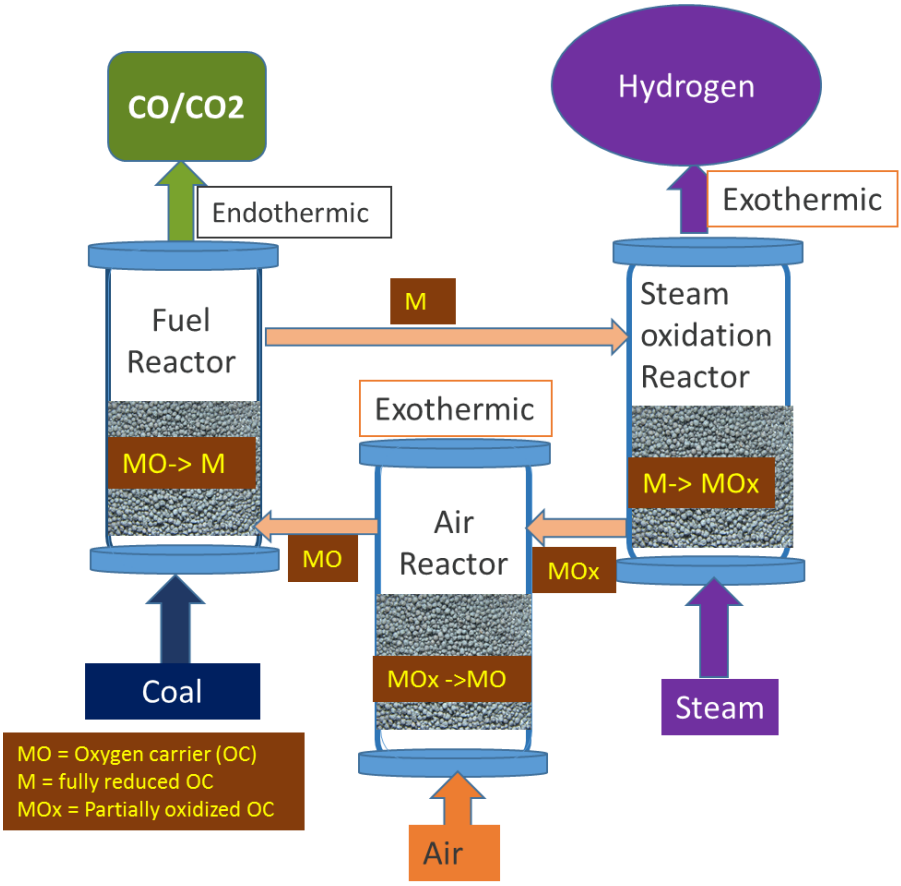

Fig 14: Process of production H_2 from steam oxidation of reduced Ca ferrite followed by air oxidation

CONCLUSIONS

Coal gasification with a $CaFe_2O_4$ oxygen carrier was demonstrated with several types of coals. Sub-bituminous and lignite coals reacted well, but the reactivity of bituminous coal was slower. Wyodak coal, PRB coal, Mississippi coal and Texas coal reacted with $CaFe_2O_4$ oxygen carrier during the temperature ramp from ambient to 850 °C to produce a CO-rich gas stream. The reduced $CaFe_2O_4$, after the reaction with coal, was oxidized with steam to produce H_2. A ten-cycle test conducted with Wyodak coal-$CaFe_2O_4$ showed stable H_2 production when steam was introduced at 800 °C. Stable H2 production was also observed during a 25-cycle steam oxidation test after reduction of Ca-ferrite with lignite coal. Scaling up the preparation process using the wet

agglomeration method was successful. Data on the production of CO with the large-scale sample $CaFe_2O_4$ and Wyodak coal was very similar to the small-scale samples. Hydrogen production during steam oxidation was demonstrated with the large-scale batch of $CaFe_2O_4$ after reduction with Wyodak coal-steam. The formation of $Ca_2Fe_2O_5$ phase was identified by XRD after steam oxidation. Kinetic analysis of steam oxidation during H_2 production indicated oxidation followed the linear rate law and oxide scale provides no resistance to diffusion pathway for oxidizing gas. Possible processes for heat integration without any CO_2 emissions are also discussed.

REFERENCES

1. Stiegel, G.J. and Ramezan, M. “Hydrogen from coal gasification: An economical pathway to a sustainable energy future,” International Journal of Coal Geology, vol. 65, pp. 173-190, 2006.
2. Sircar, S. and Golden, T.C. “Purification of hydrogen by pressure swing adsorption” Separation Science and Technology, 35, pp 667-687, 2006.
3. Chiesa, P.; Consonni, S.; Kreutz, T. and Williams, R., "Co-production of hydrogen, electricity and CO2 from coal with commercially ready technology. Part A: Performance and Emissions," International Journal of Hydrogen Energy, vol. 30, pp. 747-767, 2005.
4. Higman, C. and Van der Burgt, M., Gasification 2nd edition, p 257, Gulf Professional Publishing (Elsevier), 2008.
5. Smith A.R. and Klosek, J.,"A review of air separation technologies and their integration with energy conversion processes," Fuel Processing technology, vol. 70, pp. 115-134, 2001.
6. Guo, Q; Hu, X.; Liu, Y.; Jia, W.; Yang, M; Wu, M; Tian, H. and Ryu, H, "Coal Chemical-looping gasification of Ca-Based oxygen carriers decorated by CaO," Powder Technology, vol. 275, pp. 60-68, 2015.
7. Guo, Q; Cheng, Y.; Liu, Y; Jia, W and Ryu, H., "Coal chemical looping gasification for syngas generation using an iron-based oxygen carrier," Ind. Eng. Chem. Res., vol. 53, pp. 78-86, 2014.
8. Wei, G; He, F.; Zhao, Z; Huang, Z; Zheng, A; Zhao, K and Li,H., "Performance of Fe-Ni bimetallic oxygen carriers for chemical looping gasification of biomass in a 10 kWth interconnected circulating fluidized bed reactor," International Journal of Hydrogen Energy, vol. 40, no. 46, pp. 16021-16032, 2015.

9. Liu, Y.Z. and Guo, Q.J., “Investigation into syngas generation from solid fuel using CaSO4-based chemical looping gasification process,” Chinese Journal of Chemical Engineering, 2013;21:127-134.
10. Liu, Y.Z.; Guo, Q.J.; Cheng, J. and Ryu, H.J., “Reaction mechanism of coal chemical looping process for syngas production with CaSO4 oxygen carrier in the CO2 atmosphere,” I&EC research, 2012;51:10364-10373.
11. White, J.H.; Schutte, E.J. and Rolfe, S.L. Cyclic catalytic upgrading of chemical species using metal oxide materials. WO Patent 2008/036902 A2, 2008.
12. Lim, H.S.; Dohyung, K and Jae, W.L., “Phase transition of Fe2O3–NiO to NiFe2O4 in perovskite catalytic particles for enhanced methane chemical looping reforming-decomposition with CO2 conversion,” Applied Catalysis B: Environmental, 2017; 201: 175–183.
13. Sarafraz, M.M.; Jafarian, M; Arjomandi, M. and Nathan, G.J. “Potential use of liquid metal oxides for chemical looping gasification: A thermodynamic assessment,” Applied Catalysis B: Environmental, 2017; 202:175–183.
14. Li, S.; Xiang, D.; Xu, Y; Sun, Z. and Cao, Y. “Relationship between electronic properties of Fe3O4 substituted by Ca and Ba and their reactivity in chemical looping process: A first-principles study,” Applied Energy, 2017; 202:550–55.
15. Chen, L.; Yang, L.; Liu, F.; Nikolic, H.S.; Fan, Z. and Liu, K. “Evaluation of multi-functional iron-based carrier from bauxite residual for H2-rich syngas production via chemical-looping gasification,” Fuel Processing Technology, 2017; 156 :185–194

16. Siriwardane, R.; Riley, J; Tian, H and Richards, G, "Chemical looping coal gasification with calcium ferrite and barium ferrite via solid-solid reactions," Applied Energy, vol. 165, pp. 952-966, 2016.
17. Fan, L.S.; Zeng, L. and Luo, S. (2015), Chemical-looping technology platform. AIChE J., 61, No.1, pp.2–22., 2015 doi:10.1002/aic.14695.
18. Riley, J.; Siriwardane, R.; Tian, H.; Benincosa, W; and Poston, J., "Kinetic analysis of the interactions between calcium ferrite and coal char for chemical looping gasification applications: Identifying reduction routes and modes of oxygen transfer," Applied Energy 201 (2017) 94–110.
19. Chopra, S. and Kr Jain, A., "A review of Fixed Bed Gasification Systems for Biomass," Agricultural Engineering International: CIGRE Journal, vol. IX, no. Invited Overview No. 5, pp. 1-23, 2007.
20. Higman, C.; Van der Burgt, M. (2008). Gasification, 2nd Edition, Gulf Professional Publishing, eBook ISBN: 9780080560908.
21. Chen, L.; Bao, J.; Kong, L.; Combs, M.; Nikolic, H.; Fan, Z. and Liu, K., "The direct solid-solid reaction between coal char and iron-based oxygen carrier and its contribution to solid-fueled chemical looping combustion," Applied Energy, vol. 184, pp. 9-18, 2016.
22. Siriwardane, R.; Tian, H.; Miller, D.; Richards, G.; Simonyi, T. and Poston, J., "Evaluation of the reaction mechanism of coal-metal oxide interactions in chemical looping combustion," Combustion and Flame, vol. 157, pp. 2198-2208, 2010.
23. Richter, H.J. and Knoche, K.F., "Reversibility of combustion process," ACS Symposium Series 1983;235:71-85.

24. Ishida, M and Jin, H., "A novel combustor based on chemical-looping reactions and its reaction kinetics," Journal of Chemical Engineering of Japan 1994;27:296–301.
25. Adanez, J.; Abad, A.; Garcia-Labiano, F.; Gayan, P. and Diego, L., "Progress in Chemicals-looping combustion and reforming technologies," Progress in Energy and Combustion Science 2012;38:215−282.
26. Lyngfelt, A., "Chemical looping combustion of solid fuels – Status and development," Applied Energy, 2014;113:1869-1873.
27. Fan LS. Chemical looping systems for fossil energy conversions. John Wiley and Sons Inc.; 2010.
28. Anthony, EJ., "Solid looping cycles: a new technology for coal conversion," Industrial & Engineering Chemistry Research, 2008;47:1747.
29. Sahir, A.; Dansie, J.; Cadore, A.; and Lighty, J., "A comparative process study of chemical-looping combustion (CLC) and chemical-looping with oxygen uncoupling (CLOU) for solid fuels," International Journal of Greenhouse Gas Control, 2014;22:237-243.
30. Cao, Y and Pan, W.P., "Investigation of chemical looping combustion by solid fuels. 1. Process analysis," Energy Fuels, 2006;20:1836–1844.
31. Siriwardane, R.; Benincosa, W.; Riley, J.; Tian, H and Richards, G., "Investigation of reactions in a fluidized bed reactor during chemical
looping combustion of coal/steam with copper oxide-iron oxide-alumina oxygen carrier H2 from coal," Applied Energy, 183 (2016) 1550–1564.

32. Hurst S., “Production of hydrogen by the steam-iron method,” J Am Oil Chem Soc., 1939;16:29–36.

33. Tong, A; Sridhar, D.; Sun, Z.; et al., “Continuous high purity hydrogen generation from a syngas chemical looping 25kWth sub pilot unit with 100% carbon capture,” Fuel, 2012;103:495–505.

34. Li, F.; Zeng, L. and Fan, L.S., “Techno-economic analysis of coal-based hydrogen and electricity cogeneration processes with CO2 capture,” Ind Eng Chem Res., 2010;49: 11018–11028.

35. Aziz, M.; Zaini, I.N.; Oda, T.; Morihara, A.; Kashiwagi, T., “Energy conservative brown coal conversion to hydrogen and power based on enhanced process integration: Integrated drying, coal direct chemical looping, combined cycle and hydrogenation,” International Journal of H2 Energy, 2017; 42:2904-2913.

36. Tao Liu, T. Shunxuan Hu S, Zhongliang Yu Z, Jiejie Huang J, JiaZhou Li JZ, Zhiqing Wang Z, Yitian Fang Y., “Research of coal-direct chemical looping hydrogen generation with iron-based oxygen carrier modified by potassium,” International Journal of H2 Energy, 2017; 42:1038-1046

37. D.J. Young, High Temperature Oxidation and Corrosion of Metals, Elsevier, 2008, http://dx.doi.org/10.1016/S1875-9491(08)00010-0.